Journal of Hydrology 594 (2021) 125952

Contents lists available at ScienceDirect

Journal of Hydrology

journal homepage: www.elsevier.com/locate/jhydrol

Research papers

Impacts of agricultural topdressing practices on cyanobacterial bloom phenology in an early eutrophic plateau Lake, China

Shangbo Yang [a], Xiaoling Chen [a], Jianzhong Lu [a,*], Xuejiao Hou [b], Wenkai Li [a], Qiangqiang Xu [a]

[a] State Key Laboratory of Information Engineering in Surveying, Mapping and Remote Sensing, Wuhan University, Wuhan 430079, China
[b] Department of Physical Geography, Utrecht University, Utrecht, the Netherlands

ARTICLE INFO

This manuscript was handled by Huaming Guo, Editor-in-Chief, with the assistance of Rafael Perez Lopez, Associate Editor

Keywords:
Cyanobacterial bloom
Phycocyanin pigment
Phenology metrics
Agricultural topdressing practices
Erhai lake

ABSTRACT

Agricultural practices-induced pollution runoff has been widely acknowledged to be a significant source of nutrients fueling cyanobacterial bloom. The impact of topdressing activities on cyanobacterial bloom phenology (key parameters for depicting bloom process), however, has not been verified. Taking Lake Erhai, a typical eutrophic plateau lake, as an example, this study explored the spatio-temporal characteristics of phenological metrics and coverage extent for surface cyanobacterial bloom, based on phycocyanin pigment series retrieved from satellite and investigated the bloom responses to environmental forces. The results showed that higher intensity and earlier onset bloom with a larger coverage extent mainly occurred in the northern region. We identified three distinct cyanobacterial bloom growth patterns with large inter-annual variability in their bloom initiation timing (BIT). The earlier BIT is highly linked to elevated total nitrogen level and decreased wind speed. The bloom amplitude is mainly related to summer TN in 2003–2011, while associated with winter TN/TP ratio (TN, total nitrogen; TP, total phosphorus) during 2016–2019. Additionally, we found direct evidence linking agricultural topdressing and the BIT of a typical autumn bloom. After one week for the topdressing practice, the BITs lagged by approximately average 23 days, coinciding with high rainfall intensity. Our research demonstrates the topdressing activity should be reduced through agricultural planting adjustments. High TN and TP loss crops should be prohibited; planting adjustments should decrease high TP loss crop plantings in response to regional environmental forces.

1. Introduction

Overuse of chemical fertilizers (e.g., nitrogen and phosphorus) in intensive production related to the global expansion of industrialized agriculture and the intensification of conventional agricultural practices has resulted in increased runoff and subsequently a high level of water pollution into aquatic ecosystems (Beman et al., 2005; Huisman et al., 2018). This induces eutrophication and frequently occurrence of cyanobacterial bloom in water bodies (Guan et al., 2020; O'Neil et al., 2012), further posing severe environmental and ecological problems for inland waters.

Understanding the critical temporal points during the cyanobacteria growth season could uncover the workings of the bloom process, not merely the temporally associated bloom frequencies (Mishra et al., 2019). The initiation date, peak timing, and amplitude of cyanobacterial blooms are used to define the phenology of cyanobacterial bloom (Palmer et al., 2015). Long-term monitoring of cyanobacterial bloom phenology will significantly improve our understanding of the driving mechanism behind these cyanobacterial blooms (Huisman et al., 2018; Huang et al., 2020). Moreover, this knowledge could suggest effective means for controlling blooms related to human impacts on the environment (Paerl and Barnard, 2020). However, lack of long-term on-site measurements of cyanobacteria in traditional methods presents difficulties in quantifying the cyanobacterial bloom phenology.

Satellite remote sensing providing favorable spatial and temporal coverage has exhibited as an extractive tool for investigating long-term cyanobacterial bloom phenology (Hu et al., 2010). Previous researches have applied remote sensing technology to quantify cyanobacterial bloom phenology based on an intermediary such as floating Algal index (FAI), and chlorophyll-a (Chla) pigment. In particular, Chla is a universal index for all phytoplankton, while the FAI is generally to characterize the intense cyanobacterial blooms or surface floating algae scums (Hu et al., 2010). However, little research to date has utilized cyanobacterial phycocyanin pigment (PC) concentration as an

* Corresponding author.
E-mail address: lujzhong@whu.edu.cn (J. Lu).

https://doi.org/10.1016/j.jhydrol.2020.125952
Received 5 September 2020; Received in revised form 20 December 2020; Accepted 29 December 2020
Available online 6 January 2021

intermediary for the quantification of cyanobacterial bloom phenology. PC is generally considered a diagnostic pigment for capturing cyanobacterial bloom (Qi et al., 2014), and a biological indicator for eutrophication than physiochemical indicators (nitrogen (N) or phosphorus (P)) which merely act as indirect indicators. Remotely sensed PC time series have great potential for investigating the temporal pattern of cyanobacteria and further qualification of cyanobacteria phenology (Palmer et al., 2015; Shi et al., 2019a, 2019b). As a proxy for cyanobacteria presence, satellite estimated PC concentration can be retrieved robustly using the PC index (PCI) algorithm, which is immune to disturbances and is not sensitive to perturbations from submerged macrophytes and other floating mats in surface water (Qi et al., 2014). Therefore, the PCI algorithm provides a solid foundation for establishing long-term records of PC products and cyanobacterial bloom phenology.

Moreover, the bloom phenology is influenced by several potential driving forces (Gittings et al., 2018; Yang et al., 2016; Sasaoka et al., 2011), such as nutrient enrichment (Shi et al., 2019a, 2019b; Duan et al., 2014) and meteorology variability (Zhang et al., 2012; Marchese et al., 2017). Among these influential factors, the lake nutrient level plays a crucial role in prompting cyanobacterial growth and dominating phytoplankton group, and relatively responsive to human intervention (Shi et al., 2017; Huo et al., 2019). Topdressing fertilization activity is the primary human intervention especially in agricultural dominated areas. Inappropriate topdressing fertilization schemes (i.e., quantity and timing) lead to excess nutrient exports via surface runoff from surrounding watersheds (Tang et al., 2012a, 2012b; Li et al., 2020).

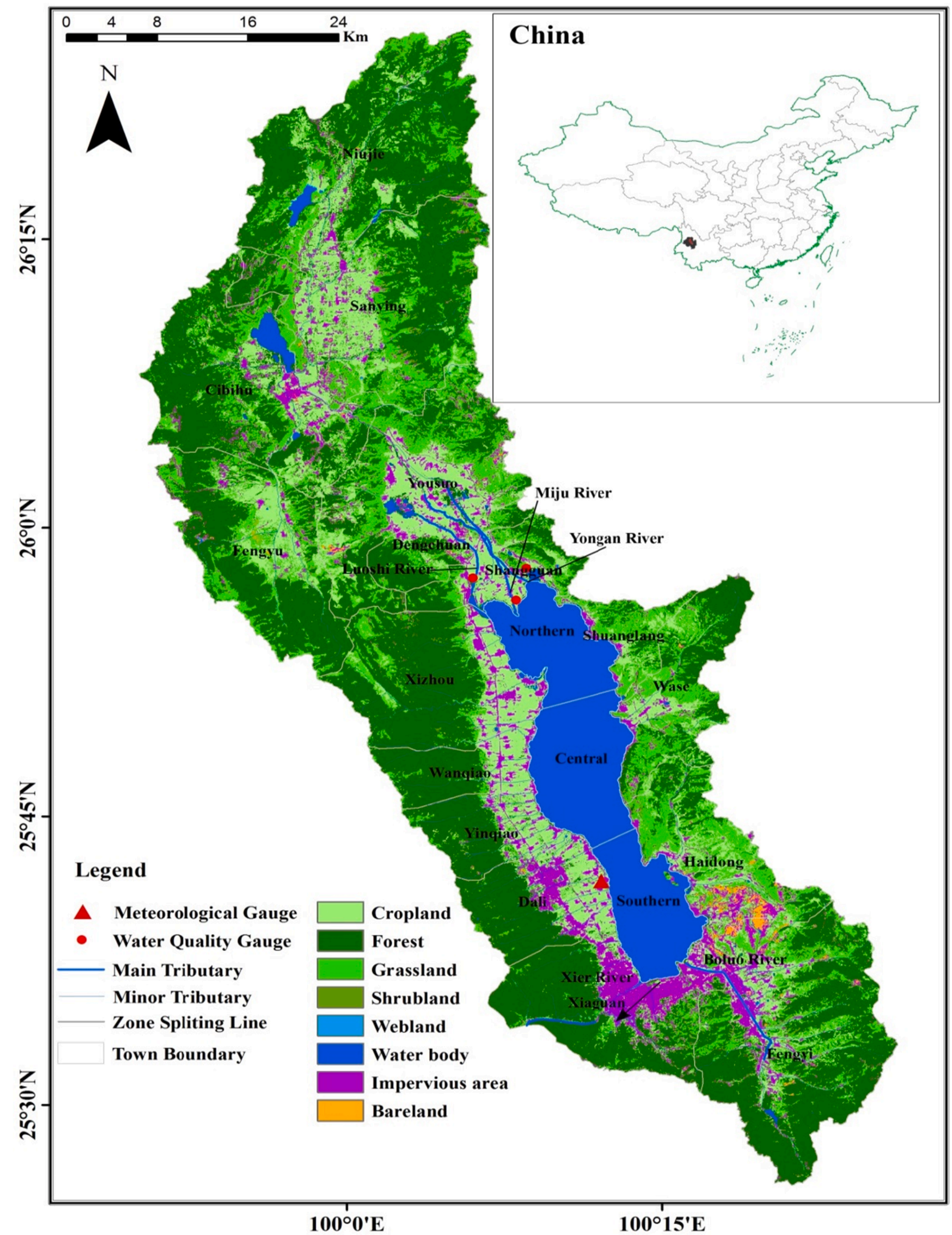

Fig. 1. An overview of the hydrological and watershed land cover (Finer Resolution Observation and Monitoring of Global Land Cover dataset) conditions of the Erhai Lake lake–floodplain system. The arrow represents the only outlet Xier River.

Agricultural planting in Erhai Lake Basin is the main reason for the water pollution of Erhai Lake (Hu et al., 2018). Lake Erhai faced with a big challenge stems from runoff from the fertilizers and pesticides applied to the surrounding farmland, and the pollution from the farmland account for at least 60% of the pollutants entering the lake (Guo et al., 2001). Even though most studies have reached a consensus that agricultural runoff could fuel phytoplankton bloom, especially in intensive farm areas, the impact of topdressing on the phytoplankton bloom phenology was not verified by observations.

This study fills this gap by linking the exogenous agriculture pollution induced by topdressing and cyanobacterial bloom phenology, thereby providing a scientific reference for agricultural planting structure adjustment. In this study, satellite estimated PC dataset was used to obtain the spatio-temporal distribution of cyanobacterial bloom features using the Gaussian fitting model and linear unmixing model during 2003–2011 and 2016–2019. Then, the bloom response to environmental factors is analyzed to uncover the driving forces of bloom dynamics. Finally, the impact of topdressing on bloom phenology was verified.

2. Material and method

2.1. Study area

Erhai Lake (25°57′-25°36′N, 100°05′-100°17′E, Fig. 1) was selected as our study area, as it is a typical semi-deep plateau freshwater lake and the main water resource for residents of Dali city in Yunnan Province of Southwestern China. This lake is considered to be in the representative preliminary eutrophic stage (Wang et al., 2015; Shang et al., 2012). The lake's total area is approximately 251 km^2. Erhai Lake has an average annual temperature of 15.1 °C and exhibits significant seasonal precipitation. In 2003–2019, about 80% rainfall was in the wet season from May to October (also the rice-growing season). Paddy rice or maize is the predominant crop in summer with the growth stages from May to September, and cultivated commonly in rotation with winter crops primarily include garlic, broad beans, oilseed rape, and wheat with the growing season from October to April (Li et al., 2018a, 2018b). There are three prominent rivers flowing into the lake, contributing to 60% of the total water inflow in the north of Erhai Lake basin. These include the Miju, the Luoshi, and the Yongan Rivers (Cao et al., 2018) which carry large-scale agricultural pollutants (Liu et al., 2019).

2.2. Data source and pre-processing

This study's primary datasets included satellite-estimated PC time series, field measurements involving phytoplankton species composition data, and auto-monitoring measurements from water quality gauges. Other data sets such as field sampling measurements extracted from Tang et al. (2012a), Tang et al. (2012b) and Liu et al. (2011), and data collected from statistical yearbooks dataset, meteorological gauge, and auxiliary monthly water environment data were also employed in this study. These data required preprocessing before they could be fed into the following analysis.

Satellite-estimated PC concentrations over periods of 2003–2011 and 2016–2019 were retrieved and validated based on the PCI algorithm according to Qi et al. (2014), using Rayleigh-corrected reflectance (Rrc) data. The Rrc datasets were obtained by using the Rayleigh Correction module embedded in Sentinel Application Platform image processor SNAP (version 7.1) to remove molecular (Rayleigh) scattering effects evident in the images collected by the Medium Resolution Instrument Sensor (MERIS) onboard the ENVISAT satellite (2003–2011) and Ocean Land Color Instrument (OLCI) on the Sentinel-3 satellite (2016–2019). Then, the Rrc dataset was used to calculate the PC index (PCI). The PCI is as follows.

$$PCI = R_{rc}^{'}(620) - R_{rc}(620) \tag{1}$$

$$R_{rc}^{'}(620) = R_{rc}(560) + \frac{620 - 560}{665 - 560} * (R_{rc}(665) - R_{rc}(560)) \tag{2}$$

The PCI is constructed here as the spectral differences between local Rrc trough at 620 nm (diagnosed distinctive absorption peak) and baseline formed between Rrc(560) and Rrc(665), which has been demonstrated a reliable index for estimating PC pigment concentrations or identifying cyanobacterial bloom (Qi et al., 2014). The estimated PC were obtained through model development and validation based on the PCI method proposed by Qi et al. (2014).

Field measurements are obtained covering different periods. Water samples (surface water and ditch water) measurements from four typical crop rotation systems in 2009 along the basins of Miju River and Luoshi River, which were arranged in lines from the north bank of Erhai Lake northwards covering all seven towns; In situ data of phytoplankton species composition were obtained from June to November (covering cyanobacteria growing season) in 2016; The daily total nitrogen (TN) and total phosphorus (TP) from the main inflow rivers during 2016–2018 were obtained from auto-monitoring water quality gauges.

Datasets were collected from statistical records compiled by government agencies. Yearly agricultural industry-related data in Dali City during 1995–2018 were derived from the statistical yearbooks of Yunnan Province; Daily meteorological datasets such as rainfall (Rainf, mm), sunshine duration (Sundur, h), wind speed (Wspd, m/s), and air pressure (Airprs, hPa) were sourced from the National Meteorological Administration of China (http://data.cma.cn) and used to calculate the corresponding monthly climatological data. Additionally, rainfall intensity (RI, mm) is here defined as monthly maximum consecutive 5-day rainfall; Auxiliary monthly datasets including water temperature (Wtemp, °C), nutrient (TN and TP, mg/L) were obtained from the Bureau of Erhai Protection and Administration of Dali.

Satellite-estimated PC time series were used for the retrieval of phenology metrics and bloom coverage. All the monthly environmental forcing data were used to calculate the corresponding seasonal mean, sub-seasonal (early, middle, late) mean data. The seasonal and sub-seasonal mean data such as TN, TP, Wtemp, Rainf, RI, Sundur, Wspd and Airprs were all included in the multi-linear regression to account for their impacts on cyanobacterial bloom phenology.

2.3. Retrieval of phenology metrics and bloom coverage

The phenology metrics and coverage were main features for characterizing cyanobacterial blooms. Fig. 2 presents a flowchart to show how the phenology features and coverage extent of cyanobacterial bloom were extracted based on the estimated in-record phycocyanin pigment (PC) time series derived from all segments of the entire lake. These include the bloom initiation timing (BIT), bloom peaking time (BPT), bloom amplitude (BA), bloom duration (BD) and bloom coverage.

The primary dataset used for phenology metrics determination is the satellite-estimated PC concentrations. The PC concentration series were obtained through model development and validation based on the PCI algorithm defined as equation (1) and (2) using Rrc products such as Rrc (620), Rrc(560), and Rrc(665), which are obtained by a preprocessing procedure followed by the approach described in Qi et al. (2014). These PC time series were then used for the preprocessing procedure.

The binning and filtering procedure reduces the effect of outliers at an appropriate temporal resolution for describing the bloom phenology. An 8-day composite PC time series was created by binning and median averaging in a preprocessing step for phenological metrics extraction in view of the limited amount of valid satellite data. Then, the resulting 8-day binned data are filtered using the Savizky-Golay approach (Palmer et al., 2015). The cyanobacterial bloom with higher amplitude and longer duration in the annual cycle is considered as the criteria for determining the primary bloom.

A Gaussian fitting procedure for extracting primary bloom phenological metrics was performed. Given the condition that secondary

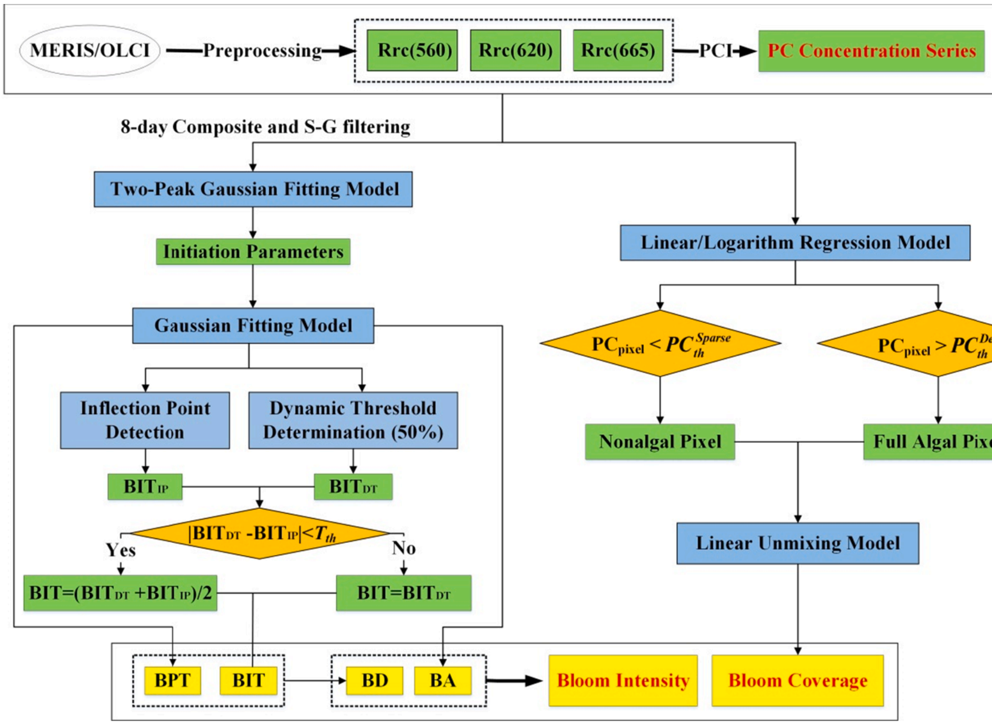

Fig. 2. Flowchart to reveal each step of the approach presented in this study. Note that BIT, BPT, BD, and BA correspond to bloom initiation timing, bloom peaking time, bloom duration, and bloom amplitude.

bloom may occur in addition to primary bloom in an annual period, a two-peak Gaussian function (Eq. (3)) for describing two-peak characteristics of the annual bloom was fitted to the filtered composite PC dataset and subsequently, the baseline of phenological metrics for the primary bloom was extracted. To increase the goodness of the phenological fitting procedure, the baseline of metrics from the identified primary bloom was then taken as initiation parameters for further adjusted Gaussian fitting (Eq. (4)) based on the algorithm proposed by Park et al. (2019). The best-fitted parameters were finally obtained using the least-squares method through the iterated procedure.

$$C(x) = C_0 + \sum_{i=1}^{2} h_i \times exp(\frac{-(x - t_{pi})^2}{2\sigma_i^2}) \tag{3}$$

$$C(x) = C_0 + h \times exp(\frac{-(x - t_p)^2}{2\sigma^2}) + \frac{d}{1 + exp(\frac{-(x - t_p)}{2\sigma})} \tag{4}$$

In these two equations, C_0 is the background PC concentration (baseline PC level determined by the fitted function), h is the BA, which is the highest value of PC during the bloom event, t_p is the BPT (Date at which the PC reaches its maximum value), σ is the bloom width, x is the time step and d represents the residual PC concentration.

The BIT was determined from the fitted PC time series using two groups of methods. A threshold method and inflection point detection method were applied (Wang et al., 2019). For a dynamic threshold method, BIT_{DT} or t_i (Eq. (5)) was identified as the date when the fitted function reaches a specific percentage 50% of the annual maximum amplitude, similar to the relative threshold method of Zhai et al. (2011). Another approach for inflection point detection in the smoothed annual PC time series curve was also adopted to determine the BIT from the annual PC series. For the curvature method, the BIT_{IP} is defined as when the rate of change in PC curvature reached the local maximum, given that rapid and excessive cyanobacterial growth is commonly referred to as a 'bloom'. The average of the above two BITs was considered as the robust BIT when the difference is below 20 days.

$$t_i = t_p - 1.17\sigma \tag{5}$$

The BD is defined as the period from initiation to when the PC concentration change decreases to 50% of the amplitude, equivalent to twice the difference between BIT and BPT. Moreover, the bloom intensity map was obtained by calculating the ratio of the BA and its corresponding BD in a pixel-by-pixel procedure.

Apart from the phenological feature extraction approach, partial-pixel cyanobacteria coverage was determined based on a long-term estimated PC dataset using a linear unmixing algorithm. The method proposed by Hu et al. (2010) was employed given the linear design of PCI facilitates pixel unmixing. The preprocessing step for the unmixing algorithm determines the threshold for non-algal and full algal pixels. However, little research has taken a PC range for classifying the bloom level. Here, bloom thresholds were determined according to an empirical logarithm and piece-wise linear relationship between satellite estimated PC and in situ cyanobacteria biomass and cell density proportion among available matchups derived from water samples (N = 28). Specifically, as shown in Fig. S1, PC's ability to indicate cyanobacteria abundance proportion is reduced as the proportion of cyanobacteria abundance becomes saturated with PCs. Additionally, cyanobacteria comprising more than 80% of phytoplankton cell density were considered dominant cyanobacteria (Orr et al., 2010). Thus, when cyanobacteria constitute more than 80% of the phytoplankton cell density (above 41ug/L by PC level), this PC level is considered a threshold for sparse bloom. Meanwhile, the dense bloom threshold by PC level is defined as 334ug/L with 100% cyanobacterial biomass proportion.

Therefore, we took the PC value of pixel (PC_{pixel}) below 41ug/L and above 334ug/L as the threshold of the nonalgal pixel (PC_{th}^{Sparse}) and full algal pixel (PC_{th}^{Dense}), respectively. In between PC_{th}^{Sparse} and PC_{th}^{Dense}, PC_{pixel} is normalized to obtain the ratio of partial coverage for the corresponding mixed pixel (α_{pixel}) as follow.

$$\alpha_{pixel} = (PC_{pixel} - PC_{th}^{Sparse})/(PC_{th}^{Dense} - PC_{th}^{Sparse}) \tag{6}$$

As such, the corresponding coverage can be obtained by a pixel's coverage (0.09 km^2) multiplied by α_{pixel}. When the pixel PC value is more than $PC_{densebloom}$, the cyanobacteria coverage is considered as 0.09 km^2. The whole coverage in each image is obtained by summing all the coverage for each available pixel.

3. Results

3.1. Spatio-temporal characteristics of phenological metrics and coverage extension

Lake Erhai shows distinct spatial and temporal heterogeneity for the bloom phenology metrics (i.e., BIT and BA), especially in the northern lake. As shown in Fig. 3, the average BIT in the northern region was nine days earlier than the BIT for the entire lake. The BIT in the entire lake ranged from 179 to 327 according to the day of the year (DoY), with annual average BIT of 246. The average BIT in the entire lake was nearly the same as the average BIT in the central or southern lake. The highest BA was observed in the north region, followed by the central and south areas. As listed in Table1, the top three high BA value ranked in order of decreasing priority occurring in 2003, 2006 and 2008, with the mean value of 1419.76 μgL^{-1}, while the top three low value ranked in the same order occurring in 2018, 2005 and 2010, with the average value of 16.86 μgL^{-1}. No temporal trend was observed during 2003–2011 in the annual mean BA, while in 2016–2019 the annual average BA showed a weak declining trend. Specifically, the BA decreased apparently from 2016 (139.2ug/L) to 2018 (21.8ug/L), and rebounded 2.5 times higher in 2019 than that in 2018. The summertime BA over the period 2016–2019 remained low as compared to the other seasons (Fig. 3).

Apart from analyzing the magnitude of the BA in the inter-annual blooms, all the annual cyanobacteria growth cycles can be grouped into three dominant seasonal cycles such as 'Early Peak', 'Late Peak', and 'Winter Max', by normalizing 52 annual PC time series derived from different regions (Fig. 4). As shown in Fig. 4a, the seasonal cycle characterized by an early-season peak, with the PC value increasing from May and decreasing from its peak in June or July to a minimum in October, was labeled 'Early Peak' (average BIT reaching DoY 173). Specifically, the blooms occurring in 2003 and 2006 belong to the 'Early Peak' group with the highest average BA up to 1162.6ug/L and shortest BD reaching 62 days. The 'Late Peak' seasonal cycle (average BIT reaching DoY 173) is characterized by a summer PC minimum, then a longer, late summer or early autumn elevated period from July through October (Fig. 4b). As displayed in Fig. 4c, the seasonal cycle characterized by a weak summer PC maximum for a short period and distinct elevated levels in late autumn, then to its peak in early winter was denoted as 'Winter Max', with BIT reaching DoY 319. For example, the blooms occurring in 2016 and 2017 were grouped to the 'Winter Max' mode, with higher BA and shorter BD than the 'Late Peak' mode. These results suggest that about 70 percent of all annual PC fitting time series were labeled as the 'Lake Peak' mode or typical autumn bloom pattern, while the 'Early Peak' and 'Winter Max' mode accounted for comparably about 15% of the total. Thus, the 'Lake Peak' mode appears the primary cyanobacteria growth periods, whereas other modes seem to result from inter-annual environmental changes.

The spatial heterogeneity of bloom coverage in regions is similar to the BA's spatial heterogeneity, with the highest bloom coverage observed in the north region, followed by central and south areas

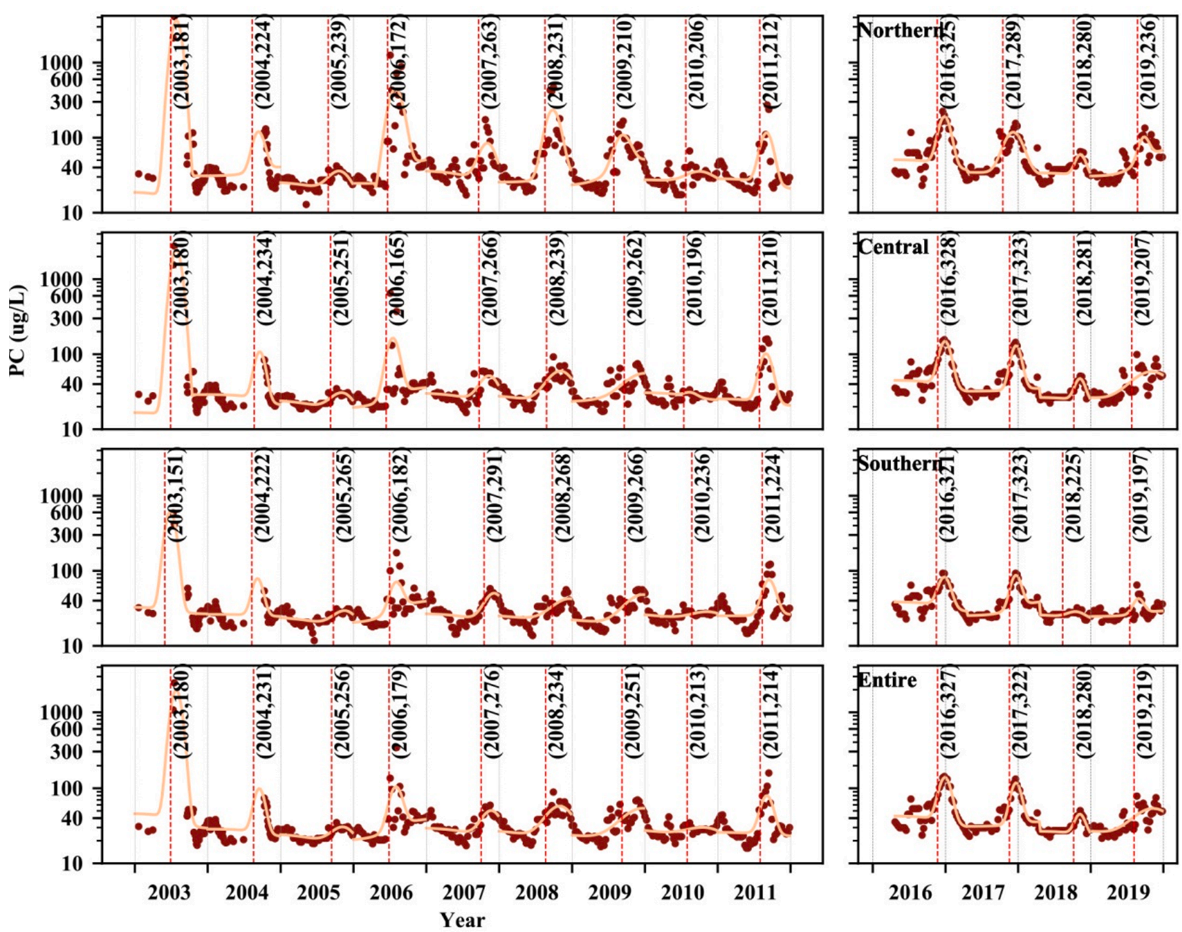

Fig. 3. Seasonal and inter-annual trends in MERIS/OLCI derived 8-day composite images of PC concentrations averaged by each region for 2003–2011 and 2016–2019, and the corresponding BITs (dotted line) derived from Gaussian curve fit.

Table 1
Phenology metrics extracted using the adjusted Gaussian fitting.

Period	C_0(μg/L)	d(μg/L)	h(μg/L)	σ(days)	t_i(days)	t_p(days)	R^2	RMSE (μg/L)	BD (days)	BC (km^2)
2003	18.81	−10.62	3633.77	25	07/28(181)	06/30(209)	0.93	201.18	56	233.73
2004	30.84	11.23	84.19	27	09/11(224)	08/11(255)	0.60	15.57	62	45.33
2005	26.32	−18.58	18.80	54	10/26(239)	08/27(299)	0.85	1.89	120	1.74
2006	4.99	50.54	419.70	34	07/30(172)	06/21(211)	0.98	22.14	78	181.03
2007	36.49	−28.28	62.10	41	11/05(263)	09/20(309)	0.96	3.79	92	52.29
2008	25.35	6.88	205.80	34	09/25(231)	08/18(269)	0.98	10.41	76	87.93
2009	22.20	34.91	68.78	38	09/10(210)	07/29(253)	0.96	5.65	86	60.41
2010	27.97	−4.89	10.02	65	10/04(206)	07/25(277)	0.53	3.10	142	7.76
2011	28.54	−8.51	92.16	29	09/02(212)	07/31(245)	0.92	8.26	66	121.26
2016	50.51	−20.37	139.22	32	12/26(325)	11/20(361)	0.95	10.05	72	163.93
2017	33.59	0.42	83.37	45	12/06(289)	10/16(340)	0.90	9.81	102	125.94
2018	32.88	3.61	21.76	26	11/05(280)	10/07(309)	0.84	3.48	58	14.37
2019	30.16	24.37	53.75	38	10/06(236)	08/24(279)	0.93	6.16	86	56.42

Note: C_0: initial PC concentration, h: BA, σ: bloom width, t_i: BIT t_p: BPT, BD: bloom duration) in Northern Lake and maximum bloom coverage (BC) in the growing season for Entire Lake.

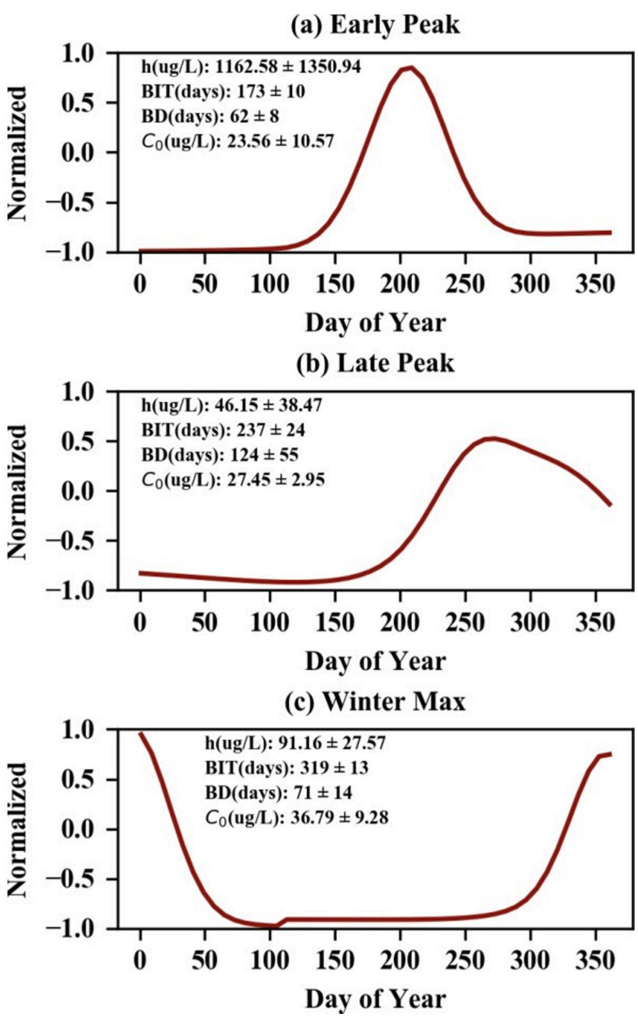

Fig. 4. Mean cyanobacteria seasonal cycles within the three groups defined by the individual annual cycles, representing phenological stages of the main cyanobacteria growth period. (a) 'Early Peak' (b) 'Late Peak' (c) 'Winter Max'. Note that the background PC concentration is denoted as C_o and the bloom amplitude is denoted as h.

(Fig. 5). As shown in Table1, during 2003–2011, the average bloom coverage area was 207.4 km^2 for BA $\geq$ 420 μgL^{-1}. Specifically, large summer blooms occurred in July 2003 and August 2006 with the maximum coverage extent of 233.7 and 181.0 km^2, respectively. In contrast, in 2016–2019, a widespread reduction in the spatial extent was particularly apparent with a trough occurring in 2018 (the maximum area of 14.4 km^2) in the growing season, and bloom coverage increased slightly in 2019 with a maximum of 56.4 km^2. In particular, winter bloom coverage reached about 163.9 and 125.9 km^2 occurring in December 2016 and 2017 (Table1). Meanwhile, the typical autumn bloom coverage has an average value of 49.7 ± 38.8 km^2.

Detailed spatial and temporal differences of the BIT and bloom intensity were shown in Fig. 6. In 2003 and 2006, the bloom occurrence was earliest with the average DoY 174 ± 9 and showed consistent spatial variation (Fig. 6a), along with the most extensive bloom coverage of 207.4 km^2 in the entire lake. In contrast, the entire lake experienced a distinct delayed BIT in 2016 and 2017 except for the northern area. Fig. 6b shows that the strongest bloom intensity was observed in the northern and central regions of Lake Erhai in 2003 (35.7 μgL^{-1}day^{-1}) and 2006 (3.0 μgL^{-1}day^{-1}). Overall, these blooms showed earlier onset and stronger intensity in the northern lake than other parts of the lake. In addition, the observed bloom intensity pattern was found to be consistent with the spatial distribution of nutrient sources obtained by Li et al. (2018a), Li et al. (2018b) and Li et al. (2020). Thus, the northern lake turns out to be an ideal location for cyanobacterial blooms owing to the effect of the surrounding agricultural activities.

3.2. Cyanobacterial bloom phenology linked with meteorological factors and lake water quality

A strengthened summer TN and weakened autumn Wspd significantly lead to an earlier onset of the blooms in the period 2003–2011. As shown in Fig. 7a, the years 2003, 2006 marked by the earlier BIT in 2003–2011. The regression results for the BIT showed that early summer TN and early autumn Wspd were the primary contributors explaining 87% of the inter-annual variation in BIT ($p < 0.01$; Table 2, Fig. 7b). It was clear that the BIT was delayed in the period 2003–2011 when summer TN decreased and autumn Wspd increased simultaneously. According to this relationship, the impact of the TN and Wspd on the BIT was quantitatively estimated, considering their contribution and variability, as presented in Fig. 7c. The BIT was delayed by about 91 days in 2007 as compared to the BIT in 2006, while the bloom occurred around 43 days later in 2004 than in 2003. The decrease of TN in 2006–2007 is similar to that in 2003–2004, which is 0.23 and 0.24 mg/L, respectively. In contrast, the increase of Wspd (0.2 m/s) in 2006–2007 was four times that in 2003–2004 (0.05 m/s). The decrease in the combined effect of the TN and Wspd during 2006–2007 was just half than that during 2003–2004. These results show that although the wind speed increased greatly and TN decreased little between the two periods, the joint interpretation of TN and Wspd decreased not that much because TN alone could account for 60% of the variability of BITs.

In contrast, low late summer Wspd significantly leads to earlier cyanobacterial bloom onset for period 2016–2019 based on the

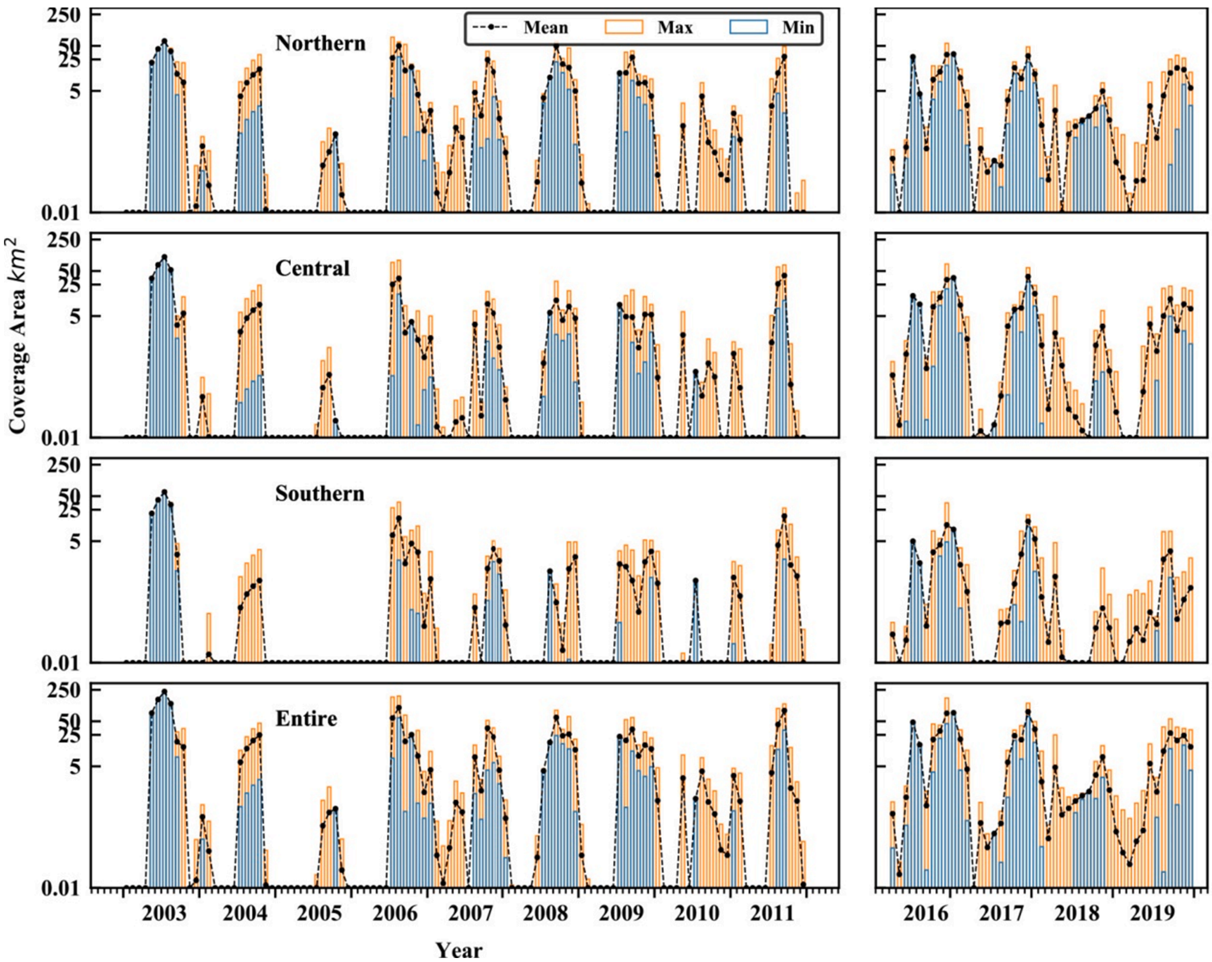

Fig. 5. Monthly coverage areas of cyanobacterial bloom for the entire lake and each segment for 2003–2011 and 2016–2019.

regression result. As shown in Fig. 7d and Fig. 7e, an advance trend of the bloom was noticeable with reduced Wspd (~ -30 days year^{-1}, $p < 0.05$). The linear regression for the BIT shows that late summer Wspd explained up to 93.5% of the observed total variation in the BIT ($p < 0.05$; Table 2, Fig. 7f). Indeed, low wind speed plays a prerequisite role in forming cyanobacteria surface cyanobacteria aggregation, especially when the wind speed is <3–4 m/s (Zhang et al., 2012). The effect of wind speed on bloom phenology is also revealed by Zhang et al. (2012) and Shi et al. (2019a), Shi et al. (2019b) that low wind speed could advance cyanobacterial bloom in Lake Taihu.

The inter-annual BIT variances were grouped according to the bloom type to explore their seasonal responses to potential environmental factors. As presented in Fig. 8, the Wtemp and Sundur exhibit a distinct correlation with the BIT variance. This indicates that the BIT was delayed significantly with the decrease in late summer sunshine hours ($r = -0.76$, $p < 0.05$) and with the warmer water temperature in early autumn ($r = 0.71$) (Fig. 8). In particular, the negative relation between the BIT and sunshine hours was also found by Zhang et al. (2012), indicating that elevated light duration promotes cyanobacteria dominance. Also, the results suggest that blooms occurring in summer generally witnessed lower early autumn Wtemp, while blooms occurring in winter were subject to a higher early autumn Wtemp in the Lake Erhai area. Especially for bloom occurrence in winter, cyanobacterial bloom onset in winter is related to the increase in water temperature (Trombetta et al., 2019).

The regression result for the bloom amplitude (BA) and environmental factors suggests that the TN appears to be the primary nutrient fueling the bloom in 2003–2011, while TN/TP ratio became the main factor prompting the bloom in 2016–2019. For instance, as for the BA in 2003–2011, the summer TN and rainfall intensity (RI) explained 61.9% and 24.7% of the BA variation ($p < 0.01$; Table 2), indicating that the enhanced amplitude is significantly correlated with both increased summer TN and RI. Moreover, cyanobacterial species without N-fixing ability (i.e., microcystis) were found to generally dominate in summer and autumn and form the bloom (Yu et al., 2014). In addition, the increase in TN level is likely to induce cyanobacterial bloom. Therefore, the relationship between TN and the BA in 2003–2011 has more to do with the rising TN driving increased cyanobacterial bloom rather than the N-fixing cyanobacteria (i.e., Anabaena) producing a large amount of TN by fixing nitrogen in the atmosphere. In contrast, winter TN/TP ratio in 2016–2019 accounted for 91.3% of the BA variations and is negative with bloom amplitude, suggesting bloom amplitude tended to increase when TN/TP decreases.

3.3. Nutrient (N and P) effects of agricultural activities in Erhai lake basin

Crops vary in their N and P fertilizer rate owing to their unique fertilizer requirements. For instance, as shown in Fig. 9a, crop garlic exhibits the highest N application rate, followed by maize, while broad bean shows the highest P application rate. Meanwhile, in the northern lake basin, the three crops displayed higher sown areas than other crops with an average of 4004 hm^2, following rice which covered the largest extent. Thus, crops such as garlic, broad bean, and maize contributed to a higher risk of N and P loss.

Inter-annual variability of agricultural activities is shown in Fig. 9b,

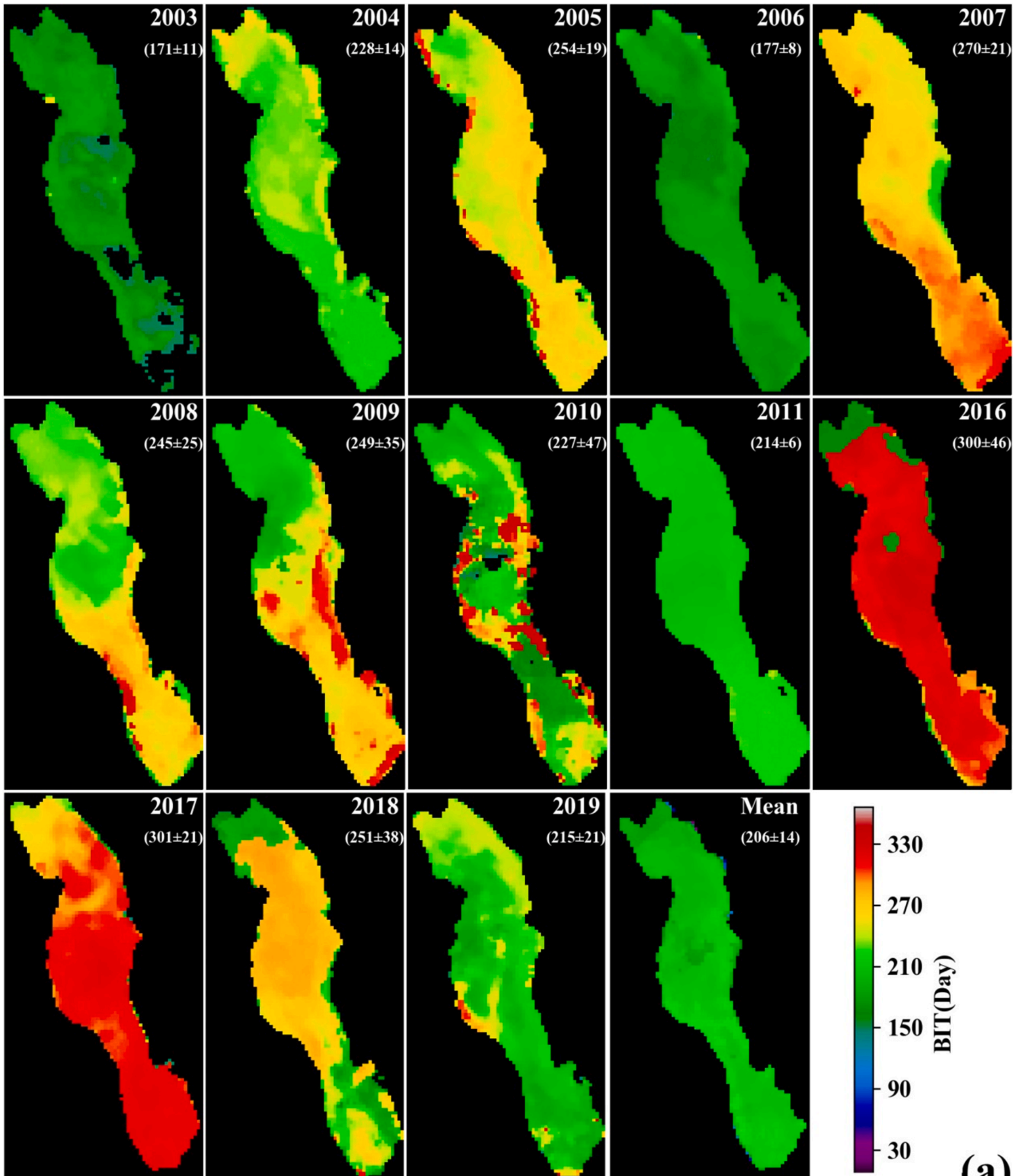

Fig. 6. Spatial distribution of annual bloom characteristics during 2003–2011 and 2016–2019. (a) BIT (mean ± stdv) (b) bloom intensity (mean ± stdv).

by depicting fertilizer amount and sown area for crop planting. As for the long-term fertilizer N and P application in Dali city, a distinct reduction occurred in 2018 following a slowly decreasing trend from 2013 to 2017, resulting from the strict control of external nutrient loadings. With regards to the sown area for crop planting, garlic cultivation was banned in the whole basin in 2018, and the beans rotated together with garlic decreased by 24.0% in the same year. In contrast, an abrupt increase in maize sown area of 15.6% was observed in 2018, followed by an increasing trend from 2009 to 2017. Additionally, the vegetable sown area in Dali city presented a significant increasing trend by 2129.1 tons year^{-1} ($p < 0.001$) from 2011 to 2018. In particular, N and P fertilizer application rates of leaf vegetables in Dali are up to 1200 and 1500 kg/hm^2 (Sun et al., 2016). Also, agricultural nonpoint source pollution mainly results from TN and TP runoff in garlic and maize lands across the northern area of Erhai Lake (Cheng et al., 2010). Accordingly, apart from garlic cultivation, other crops such as maize with high N fertilizer use, broad bean with high P use, and vegetable planting with high N and P fertilization should also be considered.

Interestingly, during 2016–2019, the bloom amplitude trough in 2018 was observed and was in coincidence with strict implemented policy for agricultural planting structure adjustment represented by the ban on garlic cultivation in the whole basin, the rotation systems of which has been demonstrated to result in highest N loss and higher P loss than other rotations (Tang et al., 2012a, 2012b; Li et al., 2018a, 2018b).

3.4. *Impact of topdressing activities on the phenological characteristics of cyanobacterial bloom*

3.4.1. *Nutrient state of three inflowing tributaries and lake Erhai*

There exists a decreasing trend in nutrients (TN and TP) of the three

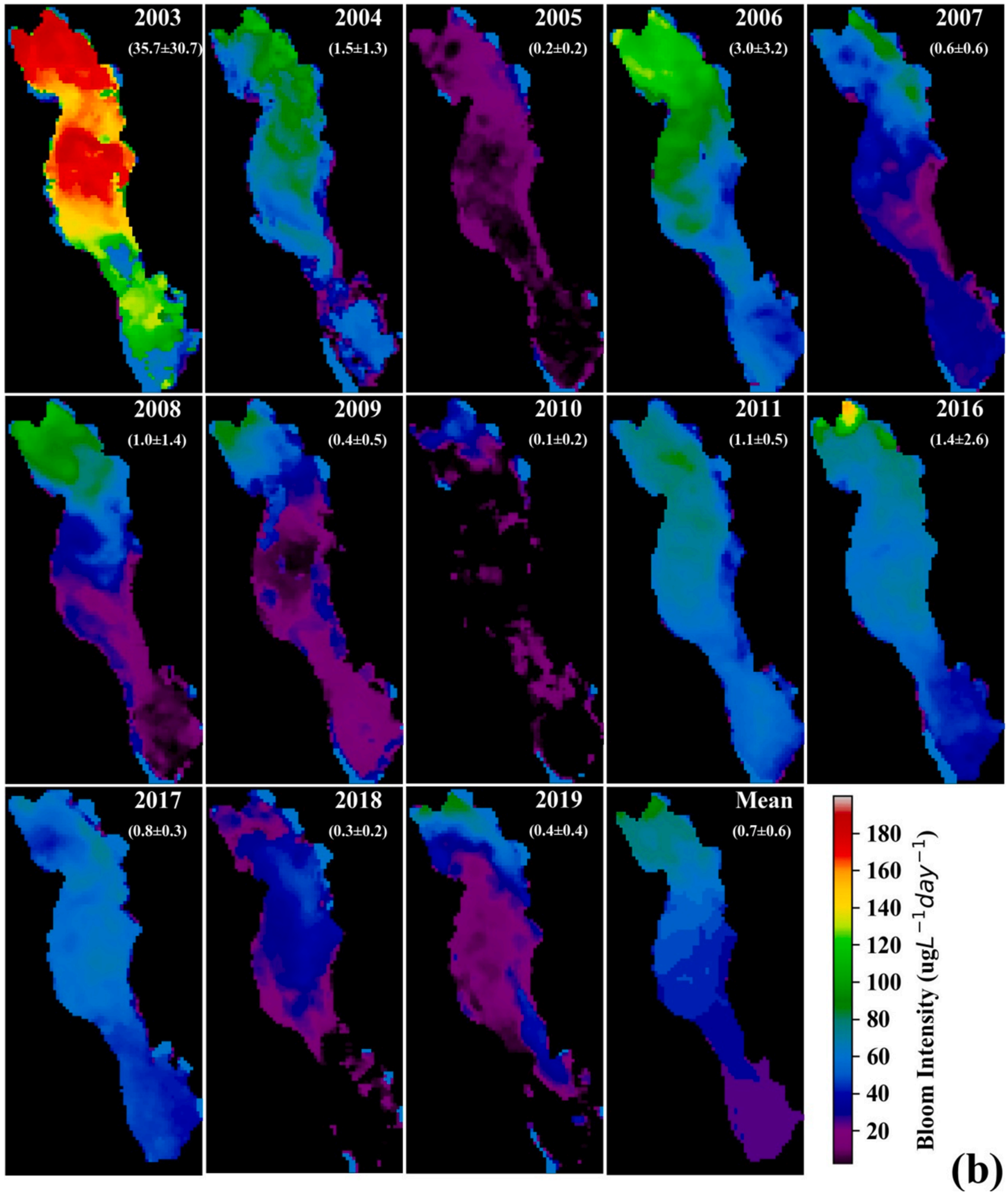

Fig. 6. (*continued*).

tributaries during Jun 2016 and Jun 2019. As shown in the upper panel of Fig. 10a, both the TN and TP levels of the Miju River (the largest inflow of lake) exhibited a slight decrease trend. A decreasing trend in TP level was both observed in Luoshi and Yongan River. Meanwhile, a marked decreasing trend in the TN level of Yongan River was observed, while the Luoshi River showed a significant increasing trend in TN level (Fig. 10a, lower and middle panel).

The distinct inter-annual and seasonal variability in TN and TP levels were observed in Lake Erhai (Fig. 10b). The annual mean TP level exhibited an apparent decrease trend in 2016–2019. The 2003–2019 TP time series showed that the TP level in summer and autumn was about 1.57 times higher than other seasons (Fig. 10b, upper panel). Specifically for the period 2016–2018, TP level in autumn and winter decreased significantly. In contrast, in 2003 and 2006, two peaks of the TN level were observed simultaneously in summer and autumn, while the TN level decreased progressively and remained at a relatively stable level of around 0.5 mg/L in all seasons after 2010, although the TN level was elevated a bit in autumn during 2016–2019 (Fig. 10b, middle panel). In general, the combined results for the nutrient state of lake and bloom dynamics indicate that summer bloom was alleviated through reasonable control of the TN level in Lake Erhai. Meanwhile, during 2016–2018, there was a decreasing trend in autumn and winter TP. This decrease in the TP level in autumn and winter alleviated the bloom in 2018 based on the link between winter TN/TP and the bloom amplitude. The autumn TP level increased once again in 2019 and probably resulted in a bit larger bloom in the autumn of 2019.

These results suggest that Lake Erhai is generally co-limited by N and P in summer and autumn, while limited by P in winter and spring. As shown in the lower panel of Fig. 10b, Lake Erhai generally exhibited N + P co-limitation in the summer and autumn, while it showed P only limitation mostly in winter and spring season following the TN/TP ratio criteria as proposed by Qin et al. (2020) for indicating potential lake

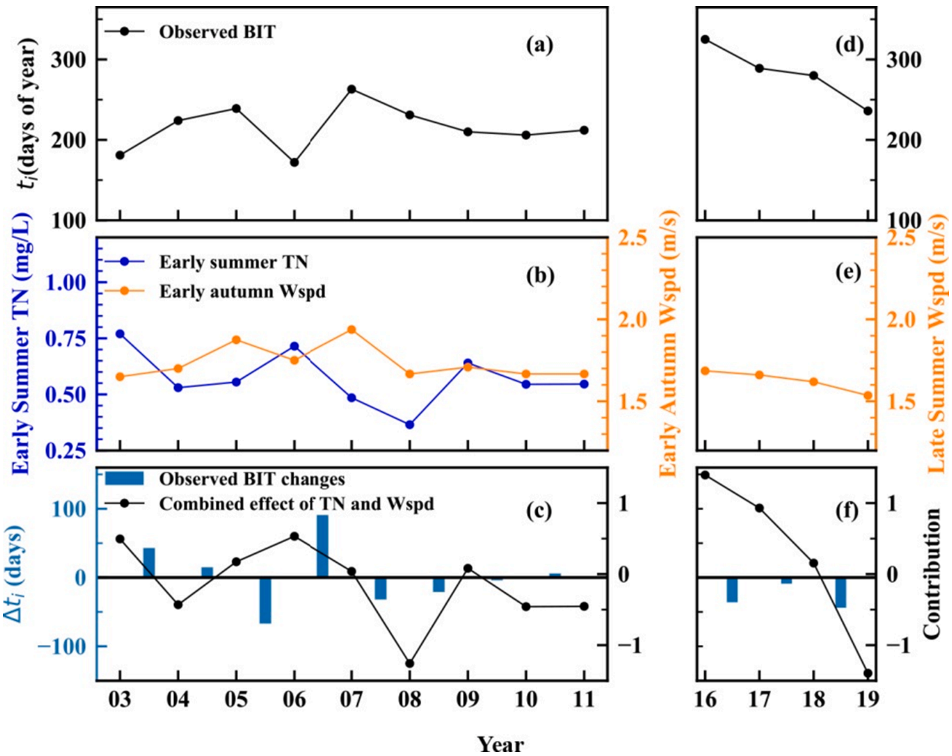

Fig. 7. Interannual variabilities in (a) The observed BIT (b) Early summer TN and early autumn Wspd during 2003–2011. (c) The time series of the observed BIT changes and the combined effect of TN and wind speed (Wspd). The vertical axis on the left represents the year-to-year differences in the observed BIT. The vertical axis on the right represents the ratio of the normalized values of TN and Wspd (i.e., 0.60× normalized TN + 0.27× normalized Wspd), showing the effect of both predictors quantitatively simultaneously. (d)-(e) the modeled BIT and late summer Wspd during 2016–2019. (f) The time series of the observed BIT changes and the effect of late summer Wspd.

Table 2
The results of multilinear (Linear) regression for primary bloom phenology features over 2003–2011 and 2016–2019.

Period	Feature	Predictor	Standardized Coefficients	*t* statistic	VIF	Relative contribution (%)	R^2	RMSE	*p* value
2003–2011	Amplitude	Summer TN	0.58	3.55*	1.18	61.92	0.87	497.4 (μg/L)	**
		Summer RI	0.54	3.33*	1.18	24.7			
	BIT	early Summer TN	−0.68	−4.52**	1.03	59.9	0.87	11.83 (days)	**
		early Autumn Wspd	0.53	3.49*	1.03	26.86			
2016–2019	Amplitude	Winter TN/TP ratio	−0.96	14.83*		91.29	0.91	18.04 (μg/L)	*
	BIT	late Summer Wspd	0.97	5.36*		93.50	0.93	11.43 (days)	*

Note: The P-value is denoted as * ($P < 0.05$), ** ($P < 0.01$), and ***($P < 0.001$); A variance inflation factor (VIF) value over 10 is a clear signal of multicollinearity.

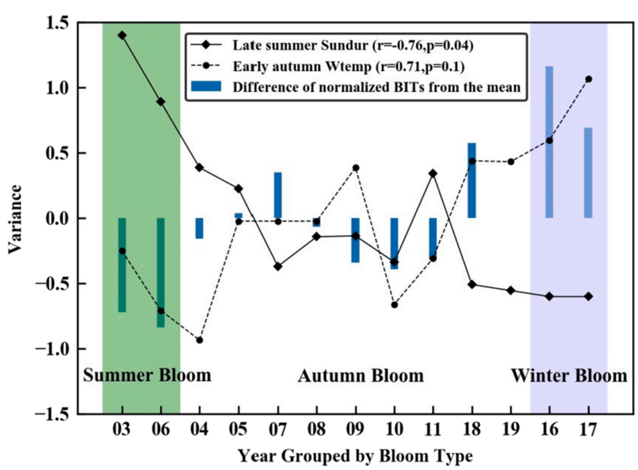

Fig. 8. Correlation between environmental variables involving Wtemp, Sundur, and the BIT variance. Note that water temperature is denoted as Wtemp and sunshine duration is denoted as Sundur; All the potential environmental variables and the BIT variance were normalized before the correlation analysis.

nutrient limitation. In particular, the summer and autumn seasons are in the rainy season, covering May to October. In this period, rice cropping was the primary agricultural activity in the Lake Erhai basin, and the fertilization application in this hot period of cropping contributes to the plenty of N and P runoff losses from intensive agricultural watersheds due to the synchrony between extreme rainfall and fertilization events, especially topdressing activities. Thus, Lake Erhai appears to limited by the fertilizer application induced nutrient runoff during cropping in the summer and autumn seasons.

3.4.2. Relationship between topdressing and phenological metrics

As shown in Fig. 11a, garlic-rice and broad bean-rice planting modes were major crop rotation systems in the northern watershed of Erhai Lake, suffering from the maximum amount of runoff TN losses and TP losses at 17.82 kg/hm^2 and 3.26 kg/hm^2, respectively. Then, garlic-rice rotation produces most runoff TN losses and relatively high TP losses. Owing to the positive relationship between nutrient N loss in farmland with fertilizer application amount (Li et al., 2018a, 2018b), the amount of chemical fertilizer application was the highest during the garlic-rice rotation.

The effect of the topdressing application on the TN and TP levels in the surface and ditch water of farmland is revealed during the second primary topdressing period from July 10th to July 15 in 2009 (Fig. 11b). A substantial increase of 74% in TP and 35% in TN was observed in cropland's surface water on the just beginning date (July 10th) of

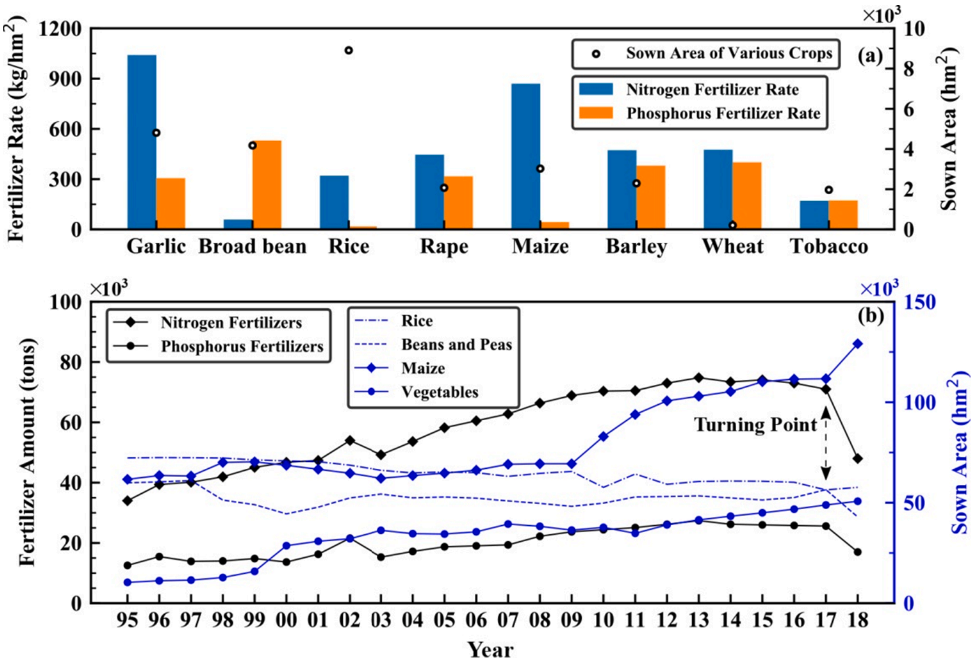

Fig. 9. The crops sown area and fertilizer application (a) The crops sown area in the year 2008 and fertilizer amount in northern lake basin obtained from Liu et al. (2011). (b) The sown area of four main crops selected with an average area of more than 30 thousand hm^2 and fertilizer amount (1995–2018) in Dali city.

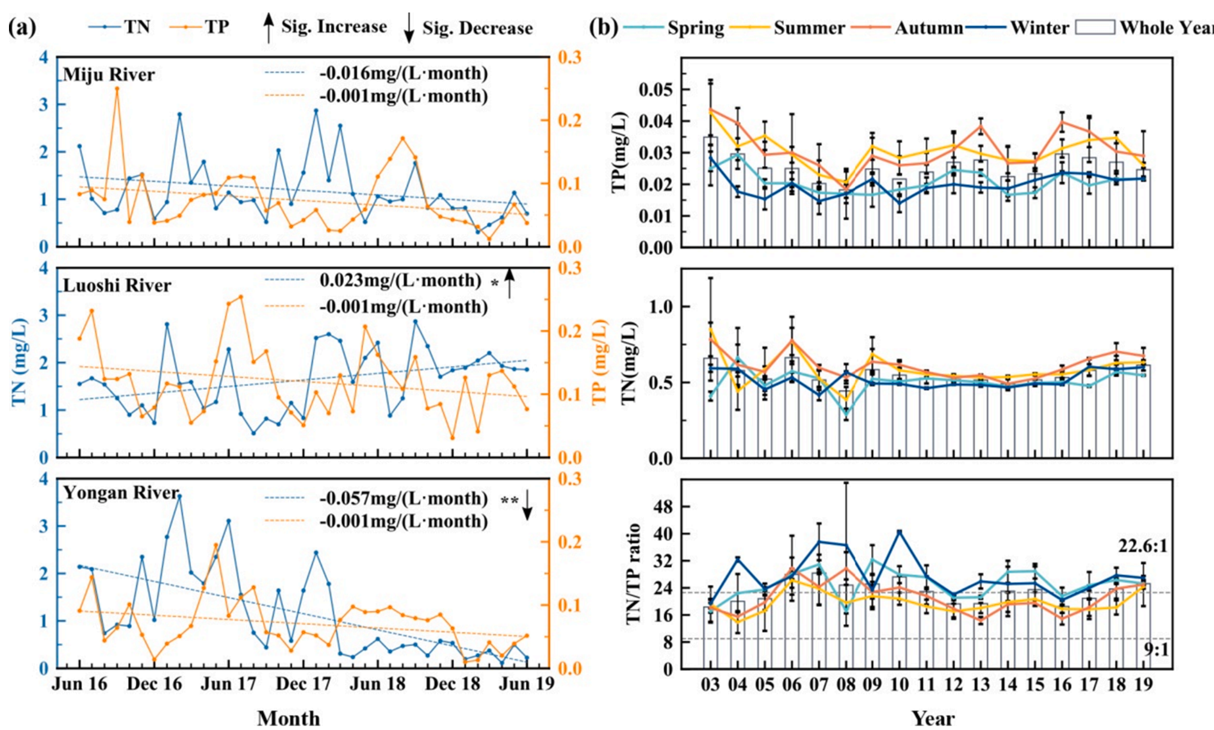

Fig. 10. Nutrient status in inflowing tributaries and surface lake (a) Monthly average nutrients TP and TN concentrations from three major tributaries including Miju, Luoshi, and Yongan River. The annotations "↑" and "↓" represent statistically significant increasing and decreasing trends, respectively, from June 2016 to June 2019. The P-value for the linear trend is denoted as * ($P < 0.05$) and ** ($P < 0.01$) (b) Temporal variations in the average nutrients involving TN, TP, TN/TP ratio in Erhai Lake during the period 2003–2019.

topdressing fertilization. About a week later than the ending date of this topdressing period, the TN and TP levels in ditch water reached their peak at 5.83 mg/L (a four-fold increase) and 0.32 mg/L (a five-fold increase) on July 21th. This was the time of the ditch nutrient peak when the rainfall reached 42.8 mm. Notably, a one-week window (seven days after fertilizer application) for each topdressing range is also optimal in this study, consistent with (Cui et al., 2020) and (Xue et al., 2014). The results suggested that surface water in cropland overflows into the surrounding ditches (acting as the major pathway of farmland surface runoff) through surface runoff after a certain amount of rainfall (rainfall reached 30 mm/d). Thus, nutrients increase in surface water of farmland and afterward in ditch water is primarily due to the amount of chemical

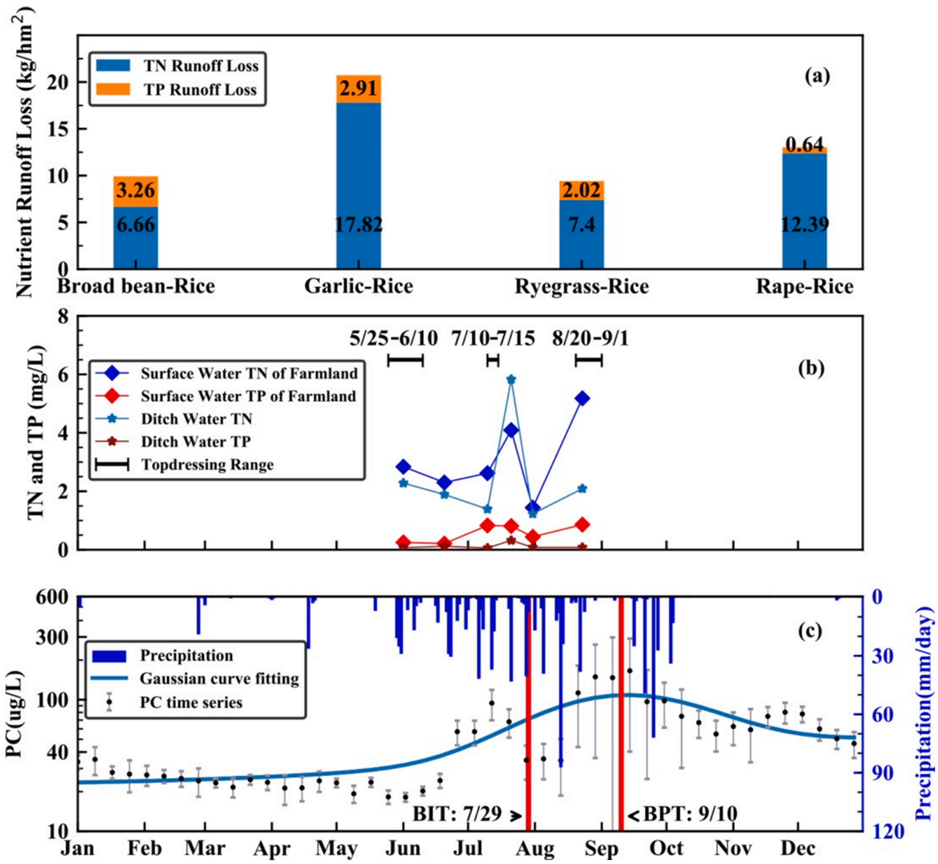

Fig. 11. The link between topdressing and BIT (a) Runoff TN and TP losses under four major planting modes (b) Surface water TN and TP of farmland and ditch water TN and TP sampled in the rice-growing season by in-field survey conducted in 2009. Three primary topdressing periods (from May 25th to June 10th, from July 10th to July 15th, from August 20th to September 1th) were obtained from household survey of fertilizer conducted by Tang et al.2012. (c) Relationship between satellites estimated PC concentrations and rainfall levels in 2009.

fertilizer application in the topdressing practices. Moreover, the timing of topdressing application turns out to be the critical period of nutrient runoff losses, especially at the critical growth stages of rice crop.

The synchrony between topdressing fertilization and extreme rainfall events indicates the high probability of N and P runoff happened during the fertilization period, providing sufficient nutrients for cyanobacterial bloom occurrence. With the introduction of satellite estimated PC time series in 2009, the effect of the topdressing application on cyanobacterial bloom phenology is revealed in Fig. 11c. The BIT of this typical autumn bloom was July 29 th, about eight days later following the ditch nutrient peak timing. This nutrient peak timing in ditch water was just the end of the one-week window before which the nearest topdressing event is finished, indicating the risk period of runoff TN and TP losses. The BPT occurred on September 10th, nine days later than the end of the third topdressing range. In particular, during the three topdressing periods from the earliest May 25th to August 20th, the days with rainfall more than 30 mm/d lasted for a week. The maximum rainfall value was 87.6 mm/d occurring on August 13th. As such, given the coincidence of such massive rainfall events, especially shortly after the topdressing activities, any remaining excess nutrients in surface water of farmland after the topdressing application entered into ditches from the ridge of field and produced runoff, then feed into nearby river channels (Miju River or Luoshi River), and finally directly flooded into the northern lake, providing sufficient nutrients for cyanobacteria growth, resulting in a rapid increase in the PC concentrations surrounding the corresponding inlet.

Further, we calculated the time lag for each BIT with ditch nutrient peak timing induced from the nearest topdressing event in the whole study period, and the distribution of time lag was presented in Fig. 12, with an average of 23 $\pm$ 18 days. The BITs for summer bloom occurring in 2003 and 2006 are close to the first primary topdressing range, indicating that the topdressing event from May 25th to June 10 provided

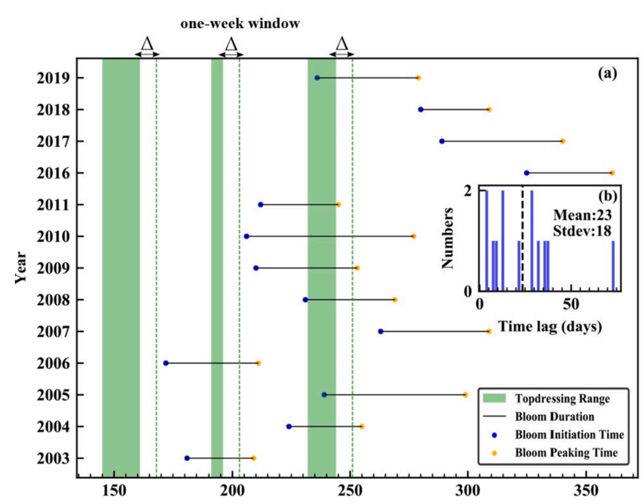

Fig. 12. The impact of long-term topdressing activities on phenological metrics (a) Links between phenological metrics (BIT, BPT) covering the whole periods and the primary topdressing ranges. (b) Histogram for time lags with dashed line represents its mean value.

a nutrient basis for summer bloom. By contrast, the time lags for winter blooms occurrence in 2016 and 2017 were relatively larger with the value 38 and 74, respectively. In particular, most BITs of autumn bloom were observed occurring close to the second topdressing period. Additionally, the time lag in the whole period was significantly positively correlated with autumn water temperature ($r = 0.6$, $p < 0.05$).

4. Discussion

4.1. Implications for environment protection in Lake Erhai

Our research shows a link between fertilizer topdressing application and cyanobacterial blooms. For example, a sharp drop in fertilizer application was highly associated with alleviated bloom in 2018. As such, mitigation strategies for addressing the ongoing challenge could be drawn from this link, as other researchers have indicated. Source control strategy aiming to reduce excess fertilizer N and P application is preferred for agricultural runoff pollution control (Zou et al., 2019; Xia et al., 2020). Accordingly, we concur that the first and foremost strategy to mitigate bloom occurrences in Lake Erhai should focus on reducing the amount and the frequency of fertilizer topdressing.

It can be inferred from the results of this study that a reduction in nutrient runoff could be realized by several approaches, such as reducing the application rate of applied fertilizer on a specific area of cropland or switching land allocation from a fertilizer-intensive crop to a fertilizer-saving crop. Indeed, switching land allocation is an effective method to optimize a reasonable planting structure and avoid high fertilizer input. For example, a shift from cultivating staple food crops requiring high-fertilizer to preferentially cultivating crops such as flowers, rapes, medicinal materials, and other crops with higher profits for producers and smaller amounts of fertilizer additions is necessary.

From the perspective of external pollution control, banning garlic planting in the whole watershed in 2018 could reduce the loss of large amount N. Although there was an unexpected increase in the TN level of Lake Erhai occurring in 2018, the TN level observed in the lake has remained at a constant low level owing to the consistent control strategy, which results in little influence on the occurrence of cyanobacteria bloom. Much efforts have been made to reduce high N export, and it turns out that high N export needs to be prohibited. However, the TP level has not been controlled. More importantly, the TP level has been demonstrated to be the primary driver for cyanobacterial bloom in Lake Erhai in recent years. Therefore, our results suggest the need to reduce conventional P fertilizer application in crop production regions, and high P loss crops in rotation crop systems (i.e., broad bean, wheat) should be considered. Strictly bans stimulate adjustment of planting structure, which in turn affects fertilizer use. In particular, typical fertilizer-intensive crops, including maize and leaf vegetables, are increasingly cultivated over wider areas of land in the study area. Under such a cultivation trend, the P management strategy should be strengthened. The consistent suggestion could also be found in Fan et al (2020).

4.2. Uncertainty and limitations

The mutation feature of bloom in a shorter period observed by satellite would bring uncertainty in PC time series analysis procedures such as 8-day PC composition and the Savizky-Golay approach. Although MERIS/OLCI provides an ideally revisit time of three days at the equator in cloud-free conditions, the actual temporal resolution of available image series in this research is limited with an average of 4.7 ± 4.8 days owing to contaminations such as high cloud cover. In addition, a uniform number of images per year are required for time series analysis. For this reason, the eight days was selected as the temporal resolution, and 8-day composite series were subsequently generated when more than one observation per 8-day bin was available in this study area, although composite median averaging would bring information loss and could not capture short-term blooms. Moreover, it would take about seven days for the cyanobacterial biomass to double and dominated the phytoplankton groups with a slow-growing rate of 0.1d^{-1} (Wynne et al., 2010). Therefore, 8-day PC composition is sufficient to capture the cyanobacterial bloom phenology (seasonal trend) in the growing stages of surface cyanobacteria.

The Savizky-Golay smoothing procedure would filter out the high frequency 'noise' induced by the occurrence of short-term bloom throughout the annual cycle for cyanobacteria growth, resulting in a negative impact on the Gaussian fitting process for phenology metrics extracting. However, our results suggest that though the bloom amplitude varied in the seasonal and inter-annual scale, distinct seasonal blooms with relatively high signal–noise ratio have been frequently observed in this eutrophic lake since 2003. Thus, the smoothing procedure filtering the short-term bloom would have little impact on cyanobacterial blooms with a relatively high signal–noise ratio. Moreover, the importance of observational noise would be weaker in areas with high bloom amplitude but more significant in regions with low seasonal bloom amplitude versus noise level (Ferreira et al., 2014). Therefore, the uncertainty brought by Savizky-Golay approach would not have much impact on the results.

5. Conclusions

In this study, cyanobacterial bloom phenology and its responses to environmental forces were explored in Lake Erhai. We explored the spatio-temporal characteristics of phenological metrics and coverage extent for surface cyanobacterial bloom, based on 13-year phycocyanin pigment series retrieved from satellite using Gaussian fitting and linear unmixing models during period 2003–2011 and 2016–2019. The result indicates that high intensity and early onset bloom were identified with a large coverage extent in the north lake, showing three dominant growth patterns such as 'Early Peak', 'Late Peak', and 'Winter Max' mode. This exploration of bloom phenology responses to environmental forces shows that the TN and TP were found to the most impacts on bloom amplitude. Moreover, elevated early summer TN and weakened early autumn wind speeds contributed to early-onset bloom in 2003–2011, while reduced late summer wind speed led to earlier BIT in 2016–2019. Fluctuating TP level fueled the blooms over the period 2016–2019, occurring primarily in autumn and winter as the TN level was stable and under effective control.

Evidence for the impact of fertilizer topdressing application on cyanobacterial bloom phenology in the northern watersheds was observed, indicating that given the coincidence of such massive rainfall events, especially shortly after the topdressing activities, any remaining excess nutrients in surface water of farmland after the topdressing application entered into ditches from the ridge of field and produced runoff, then feed into nearby river channels and finally provide sufficient nutrient for cyanobacteria growth in the receiving lake. Moreover, in coincidence with high rainfall intensity, the BITs lagged by approximately an average of 23 days behind a one-week window for the topdressing practice.

The results of this research have implications for the protection of Lake Erhai. As part of agricultural planting structure adjustment implements, strict bans on garlic cultivation in the whole basin indeed positively alleviated cyanobacterial bloom by reducing the topdressing fertilization. Moreover, adjustment of planting structure turns out to be an effective measure for reducing fertilizer topdressings. Since TN pollution has been under control, crops such as leaf vegetables and wheat with high TP loss should be reduced or eliminated. Our research verified the link between topdressing and cyanobacterial bloom in such a typical early eutrophication plateau lake. This would help guide for agricultural transformation from traditional planting towards more economically and environmentally friendly practices. Similar work for reducing topdressing activities during sensitive periods for cyanobacterial bloom and optimizing planting structure could also be implemented in other agricultural planting dominated areas.

Declaration of Competing Interest

The authors declare that they have no known competing financial interests or personal relationships that could have appeared to influence the work reported in this paper.

Acknowledgements

This work was funded by the National Natural Science Foundation of China (41971402), the Frontier Project of Applied Foundation of Wuhan (2019020701011502), the Natural Science Foundation of Hubei Province (2019CFB736), Key Research and Development Program of Jiangxi Province (20201BBG71002), the ESA-MOST Dragon Program, and the LIESMARS Special Research Funding. We thank the Bureau of Erhai Protection and Administration of Dali for providing monthly datasets including water temperature, nutrient (TN and TP), and Dr. Yongmin Qiao of Jinan University for providing the phytoplankton species composition data. We also thank the editor and two anonymous reviewers for their suggestions for this manuscript.

Appendix A. Supplementary data

Supplementary data to this article can be found online at https://doi.org/10.1016/j.jhydrol.2020.125952.

References

Beman, J.M., Arrigo, K.R., Matson, P.A., 2005. Agricultural runoff fuels large phytoplankton blooms in vulnerable areas of the ocean. Nature 434 (7030), 211–214.

Cao, J., Hou, Z., Li, Z., Chu, Z., Yang, P., Zheng, B., 2018. Succession of phytoplankton functional groups and their driving factors in a subtropical plateau lake. Sci. Total Environ. 631–632, 1127–1137.

Cheng, L., Yin, C., Hu, W., Zhou, Y., 2010. Subsidy policy for agricultural nonpoint pollution control in Northern Area of Erhai Lake of Yunnan Province. Res. Agric. Modern. 31 (4), 471–474.

Cui, N., Cai, M., Zhang, X., et al., 2020. Runoff loss of nitrogen and phosphorus from a rice paddy field in the east of China: Effects of long-term chemical N fertilizer and organic manure applications. Global Ecology and Conservation 22 (e01011).

Duan, H., Ma, R., Zhang, Y., Loiselle, S.A., 2014. Are algal blooms occurring later in Lake Taihu? Climate local effects outcompete mitigation prevention. J. Plankton Res. 36 (3), 866–871.

Ferreira, A.S., Visser, A.W., MacKenzie, B.R., Payne, M.R., 2014. Accuracy and precision in the calculation of phenology metrics. J. Geophys. Res. Oceans 119 (12), 8438–8453.

Gittings, J.A., Raitsos, D.E., Krokos, G., Hoteit, I., 2018. Impacts of warming on phytoplankton abundance and phenology in a typical tropical marine ecosystem. Sci. Rep. 8 (1), 2240.

Guan, Q., Feng, L., Hou, X., Schurgers, G., Zheng, Y., Tang, J., 2020. Eutrophication changes in fifty large lakes on the Yangtze Plain of China derived from MERIS and OLCI observations. Remote Sens. Environ. 246.

Guo, H.C., Liu, L., Huang, G.H., Fuller, G.A., Zou, R., Yin, Y.Y., 2001. A system dynamics approach for regional environmental planning and management: a study for the Lake Erhai Basin. J. Environ. Manage. 61 (1), 93–111.

Hu, C., Lee, Z., Ma, R., Yu, K., Li, D., Shang, S., 2010. Moderate Resolution Imaging Spectroradiometer (MODIS) observations of cyanobacteria blooms in Taihu Lake, China. J. Geophys. Res. 115 (C4) https://doi.org/10.1029/2009JC005511.

Hu, Y., Peng, J., Liu, Y., Tian, L., 2018. Integrating ecosystem services trade-offs with paddy land-to-dry land decisions: A scenario approach in Erhai Lake Basin, southwest China. Sci. Total Environ. 625, 849–860.

Huang, J., Zhang, Y., Arhonditsis, G.B., Gao, J., Chen, Q., Peng, J., 2020. The magnitude and drivers of harmful algal blooms in China's lakes and reservoirs: A national-scale characterization. Water Res. 181, 115902.

Huisman, J., Codd, G.A., Paerl, H.W., Ibelings, B.W., Verspagen, J.M.H., Visser, P.M., 2018. Cyanobacterial blooms. Nat. Rev. Microbiol. 16 (8), 471–483.

Huo, S., He, Z., Ma, C., Zhang, H., Xi, B., Xia, X., Xu, Y., Wu, F., 2019. Stricter nutrient criteria are required to mitigate the impact of climate change on harmful cyanobacterial blooms. J. Hydrol. 569, 698–704.

Li, W., Guo, S., Liu, H., Zhai, L., Wang, H., Lei, Q., 2018a. Comprehensive environmental impacts of fertilizer application vary among different crops: Implications for the adjustment of agricultural structure aimed to reduce fertilizer use. Agric. Water Manag. 210, 1–10.

Li, Y., Liu, H., Lei, Q., Hu, W., Wang, H., Zhai, L., Ren, T., Lian, H., 2018b. Impact of human activities on net anthropogenic nitrogen inputs (NANI) at township scale in Erhai lake basin. Environ. Sci. 39 (9), 4189–4198.

Li, Y., Yen, H., Lei, Q., Qiu, W., Luo, J., Lindsey, S., Qin, L., Zhai, L., Wang, H., Wu, S., Li, W., Hu, W., Li, H., Liu, H., 2020. Impact of human activities on phosphorus flows on an early eutrophic plateau: A case study in Southwest China. Sci. Total Environ. 714, 136851.

Liu, J., Xu, J., Chen, J., Hong, X., Zhou, M., 2019. Spatio-temporal distribution characteristics of water quality in miju river and Erhai lake. J. Coastal Res. 93 (sp1), 31. https://doi.org/10.2112/SI93-005.1.

Liu, P., Lei, B., Zhai, L., Ni, X., Luo, X., Hu, W., Hongbin, L., 2011. Effects of nitrogen managements on growth of garlic and risk of nitrogen loss in field of Erhai lake basin, China. J. Agro-Environ. Sci. 30 (7), 1364–1370.

Marchese, C., Albouy, C., Tremblay, J.-É., Dumont, D., D'Ortenzio, F., Vissault, S., Bélanger, S., 2017. Changes in phytoplankton bloom phenology over the North Water (NOW) polynya: a response to changing environmental conditions. Polar Biol. 40 (9), 1721–1737.

Mishra, S., Stumpf, R.P., Schaeffer, B.A., Werdell, P.J., Loftin, K.A., Meredith, A., 2019. Measurement of cyanobacterial bloom magnitude using satellite remote sensing. Sci. Rep. 9 (1), 18310.

O'Neil, J.M., Davis, T.W., Burford, M.A., Gobler, C.J., 2012. The rise of harmful cyanobacteria blooms: The potential roles of eutrophication and climate change. Harmful Algae 14, 313–334.

Orr, P.T., Rasmussen, J.P., Burford, M.A., Eaglesham, G.K., Lennox, S.M., 2010. Evaluation of quantitative real-time PCR to characterise spatial and temporal variations in cyanobacteria, Cylindrospermopsis raciborskii (Woloszynska) Seenaya et Subba Raju and cylindrospermopsin concentrations in three subtropical Australian reservoirs. Harmful Algae 9 (3), 243–254.

Paerl, H.W., Barnard, M.A., 2020. Mitigating the global expansion of harmful cyanobacterial blooms: Moving targets in a human- and climatically-altered world. Harmful Algae 96, 101845.

Palmer, S.C.J., Odermatt, D., Hunter, P.D., Brockmann, C., Presing, M., Balzter, H., Toth, V., 2015. Satellite remote sensing of phytoplankton phenology in Lake Balaton using 10 years of MERIS observations. Remote Sens. Environ. 158, 441–452.

Park, J., Kim, J.-H., Kim, H.-C., Hwang, J., Jo, Y.-H., Lee, S.H., 2019. Environmental forcings on the remotely sensed phytoplankton bloom phenology in the central ross sea polynya. J. Geophys. Res. Oceans 124 (8), 5400–5417.

Qi, L., Hu, C., Duan, H., Cannizzaro, J., Ma, R., 2014. A novel MERIS algorithm to derive cyanobacterial phycocyanin pigment concentrations in a eutrophic lake: Theoretical basis and practical considerations. Remote Sens. Environ. 154, 298–317.

Qin, B., Zhou, J., Elser, J.J., Gardner, W.S., Deng, J., Brookes, J.D., 2020. Water depth underpins the relative roles and fates of nitrogen and phosphorus in lakes. Environ. Sci. Technol. 54 (6), 3191–3198.

Sasaoka, K., Chiba, S., Saino, T., 2011. Climatic forcing and phytoplankton phenology over the subarctic North Pacific from 1998 to 2006, as observed from ocean color data. Geophys. Res. Lett. 38 (15) https://doi.org/10.1029/2011GL048299.

Shang, X., Wang, X., Zhang, D., Chen, W., Chen, X., Kong, H., 2012. An improved SWAT-based computational framework for identifying critical source areas for agricultural pollution at the lake basin scale. Ecol. Model. 226, 1–10.

Shi, K., Zhang, Y., Qin, B., Zhou, B., 2019a. Remote sensing of cyanobacterial blooms in inland waters: present knowledge and future challenges. Sci. Bull. 64 (20), 1540–1556.

Shi, K., Zhang, Y., Zhang, Y., Li, N.a., Qin, B., Zhu, G., Zhou, Y., 2019b. Phenology of phytoplankton blooms in a trophic lake observed from long-term MODIS data. Environ. Sci. Technol. 53 (5), 2324–2331.

Shi, K., Zhang, Y., Zhou, Y., Liu, X., Zhu, G., Qin, B., Gao, G., 2017. Long-term MODIS observations of cyanobacterial dynamics in Lake Taihu: Responses to nutrient enrichment and meteorological factors. Sci. Rep. 7, 40326.

Sun, L., Gao, S., Chu, Z., Dai, W., 2016. Effects of land use on soil nitrogen, phosphorous and organic matter contents in flatland of Erhai lake basin. Res. Environ. Sci. 29 (9), 1318–1324.

Tang, Q., Ren, T., Lei, B., Zhai, L., Hu, W., Zhang, J., Lin, T., Liu, H., 2012a. Characteristics of nitrogen and phosphorus losses in different crop rotation systems in the north of Erhai Lake basin. Agric. Sci. Technol. 13 (10), 2206–2212.

Tang, Q., Ren, T., Schweers, W., Liu, H., Baokun, L., Lin, T., Zhang, G., 2012b. Study on environmental risk and economic benefits of rotation systems in farmland of Erhai Lake basin. J. Integr. Agric. 11 (6), 1038–1047.

Trombetta, T., Vidussi, F., Mas, S., Parin, D., Simier, M., Mostajir, B., 2019. Water temperature drives phytoplankton blooms in coastal waters. PLoS One 14 (4), e0214933.

Wang, S., Zhang, L.i., Ni, L., Zhao, H., Jiao, L., Yang, S., Guo, L., Shen, J., 2015. Ecological degeneration of the Erhai Lake and prevention measures. Environmental Earth Sciences 74 (5), 3839–3847.

Wang, X., Xiao, J., Li, X., Cheng, G., Ma, M., Zhu, G., Altaf Arain, M., Andrew Black, T., Jassal, R.S., 2019. No trends in spring and autumn phenology during the global warming hiatus. Nat. Commun. 10 (1), 2389.

Wynne, T.T., Stumpf, R.P., Tomlinson, M.C., Dyble, J., 2010. Characterizing a cyanobacterial bloom in Western Lake Erie using satellite imagery and meteorological data. Limnol. Oceanogr. 55 (5), 2025–2036.

Xia, Y., Zhang, M., Tsang, D.C.W., Geng, N., Lu, D., Zhu, L., Igalavithana, A.D., Dissanayake, P.D., Rinklebe, J., Yang, X., Ok, Y.S., 2020. Recent advances in control technologies for non-point source pollution with nitrogen and phosphorous from agricultural runoff: current practices and future prospects. Appl. Biol. Chem. 63 (1) https://doi.org/10.1186/s13765-020-0493-6.

Xue, L., Yu, Y., Yang, L., 2014. Maintaining yields and reducing nitrogen loss in rice–wheat rotation system in Taihu Lake region with proper fertilizer management. Environmental Research Letters 9 (115010).

Yang, Z., Zhang, M., Shi, X., Kong, F., Ma, R., Yu, Y., 2016. Nutrient reduction magnifies the impact of extreme weather on cyanobacterial bloom formation in large shallow Lake Taihu (China). Water Res. 103, 302–310.

Yu, G., Jiang, Y., Song, G., Tan, W., Zhu, M., Li, R., 2014. Variation of Microcystis and microcystins coupling nitrogen and phosphorus nutrients in Lake Erhai, a drinking-water source in Southwest Plateau, China. Environ. Sci. Pollut. Res. 21 (16), 9887–9898.

Zhai, L., Platt, T., Tang, C., Sathyendranath, S., Hernández Walls, R., 2011. Phytoplankton phenology on the Scotian Shelf. ICES J. Mar. Sci. 68 (4), 781–791.
Zhang, M., Duan, H., Shi, X., Yu, Y., Kong, F., 2012. Contributions of meteorology to the phenology of cyanobacterial blooms: implications for future climate change. Water Res. 46 (2), 442–452.
Zou, L., Falinski, K., Zhao, P., Li, S., Lu, L., Dai, M., Zhang, Y., Yost, R., Wang, J., 2019. Current fertilization practice and phosphorus loading from soils near alpine lakes of Yunnan Province, China. Agric. Sci. 10 (01), 1–16.